Microscopic description of low-lying two-phonon states: Electromagnetic transitions

D. S. Delion
National Institute of Physics and Nuclear Engineering, P.O. Box MG-6, Bucharest Măgurele, Romania

J. Suhonen
Department of Physics, University of Jyväskylä, P.O. Box 35, FIN-40351 Jyväskylä, Finland
(Received 6 November 2002; published 3 March 2003)

Microscopic description of low-lying two-phonon states in even-even nuclei is introduced. The main building blocks are the quasiparticle random-phase approximation (QRPA) phonons. A realistic microscopic nuclear Hamiltonian, based on the Bonn one-boson-exchange potential, is diagonalized in a basis containing one-phonon and two-phonon components, coupled to a given angular momentum and parity. The QRPA equations are directly used in deriving the equations of motion for the two-phonon states. The Pauli principle is taken into account by diagonalizing the metric matrix and discarding the zero-norm states. The electromagnetic transition matrix elements are derived in terms of the metric matrix. The model has been applied to the ^{106}Pd and ^{108}Pd nuclei, known to contain two-phonon structures. In spite of its simplicity, the model predicts energies and ratios of $B(E2)$ values in a reasonable agreement with the data.

DOI: 10.1103/PhysRevC.67.034301 PACS number(s): 21.60.Ev, 21.60.Jz, 23.20.Js

I. INTRODUCTION

Most of nuclei with a small ground-state deformation have low-lying spectra with a vibrational behavior. A suitable microscopic approach to describe one-phonon states in these nuclei was given long time ago in terms of particle-hole (ph) excitations within the Tamm-Dankoff approximation (TDA) [1]. The ground-state and pairing correlations, taken into account by the use of the quasiparticle random-phase approximation (QRPA), are the most important ingredients necessary to improve the description of the one-phonon vibrational states [2]. A systematic phenomenological analysis of low-lying spectra and $B(E2)$ values of even-even nuclei revealed the existence of many-phonon states [3]. The first microscopic explanations of the low-lying excited two-phonon 0^+ state in Pb isotopes was given in terms of two-particle–two-hole ($2p$-$2h$) pairing excitations [4,5]. Later on, three-phonon states were studied in terms of $3p$-$3h$ excitations in Cd isotopes [6], and even $4p$-$4h$ states were identified as some kind of α vibrations in the spectrum of ^{208}Pb [7].

Soon after this, in a series of papers by Ring and Schuck [8,9] and especially by Liotta and Pomar [10] it was recognized that these states can be microscopically described within the so-called multistep shell model (MSM). The $2p$-$2h$ excitations within this formalism are given as superpositions of products between two TDA phonons coupled to a given angular momentum and parity. The resulting equations of motion are derived using Greens function or double-commutator technique, respectively. They contain the eigenvalues of the previous TDA step.

A generalization of this method to multiphonon states is given in Refs. [11–13]. Here two methods are developed: a generalized Wick's theorem and recursive relations, in principle, equivalent to the MSM.

As an application, the structure of the multiquasiparticle states was investigated within the MSM for the Sn [14] and Pb isotopes [15]. It is also possible to use $4p$ α-like excitations within the MSM in order to describe low-lying states together with the α-decay properties. The best example is the nucleus ^{212}Po. Its low-lying spectrum can be described by a wave function of the form $^{210}\mathrm{Pb}\otimes{}^{210}\mathrm{Po}+{}^{210}\mathrm{Bi}\otimes{}^{210}\mathrm{Bi}$ [16].

This formalism is related to the quasiparticle-phonon model (QPM) used by Soloviev and collaborators [17] to study a large variety of spectra for vibrational as well as for deformed nuclei. The wave function is built in a similar way as in the MSM, but the equations of motion are derived from a variational principle. The multipole-multipole interaction allowed to write a simple secular equation, instead of a matrix to be diagonalized. In Ref. [18] it was shown that two-phonon states are strongly fragmented in deformed nuclei. An important effect of the two-phonon correlations is the fragmentation of the one-phonon giant resonance, studied in Ref. [19]. In the last years the so-called double giant dipole resonance was intensively investigated using the QPM. The most important results in this field are described, for instance, in the review paper [20] and in Refs. [21,22]. The QPM was also applied to describe the fragmentation of the low-lying scissors 1^+ mode due to the presence of the two-phonon states [23].

In a series of papers Catara and co-workers studied the anharmonic spectrum of ^{40}Ca [24] and the electromagnetic transitions of the two-phonon states [25]. The influence of the two-phonon states on heavy ion collisions was investigated, e.g., in Refs. [26,27]. Recently, Hamamoto [28] and Bertch *et al.* [29] pointed out the role of anharmonicities using some simple models.

It is also possible to extend the particle-hole basis by a direct inclusion of the $2p$-$2h$ terms within the extended QRPA [30], but the resulting equations are rather complicated. In most applications it is preferred, for the sake of simplicity, to adopt the multistep technique in which building blocks are the QRPA phonons. All these microscopic descriptions of multiphonon states, and especially the double-commutator technique to derive the equation of motion, are

actually particular realizations of the so-called boson-expansion technique [31].

In this paper we propose a simplified variant of the MSM to describe multiphonon states. It was introduced at the TDA level in the already mentioned Ref. [16]. We use directly the QRPA equations in deriving the equation of motion for a composite excitation. In this way the Hamiltonian matrix elements, connecting two-phonon components, become proportional to the metric matrix. We apply this technique to describe probably one of the most striking examples of two-phonon excitations, namely, the almost degenerate triplet of $0^+,2^+,4^+$ states in the ^{106}Pd and ^{108}Pd isotopes. We will continue to apply this method in a forthcoming series of papers aiming to describe beta and double-beta transitions, and alpha decays involving two-phonon states.

The paper is organized as follows. In Sec. II we give necessary theoretical details on the wave functions, equations of motion, and electromagnetic transitions for two-phonon states. In Sec. III we analyze the low-lying spectra and $B(E2)$ values of ^{106}Pd and ^{108}Pd nuclei, and in the last section we draw conclusions.

II. THEORETICAL BACKGROUND

A. One-phonon states

We will build two-phonon states in terms of the QRPA degrees of freedom. The QRPA is a well known method, but in order to introduce some basic notations we will remind the reader of its main ingredients. We will describe collective low-lying excitations in even-even nuclei in terms of single-particle eigenstates in a given spherically symmetric mean field. These states are labeled by spherical single-particle quantum numbers, i.e., isospin, energy eigenvalue, angular momentum, total spin, and its projection. We denote them by using the following shorthand notation

$$c^\dagger_{\tau\epsilon ljm}\rightarrow c^\dagger_{\tau jm}, \tag{2.1}$$

where j now absorbs the energy eigenvalue and orbital angular momentum l. In the following we will drop the isospin index wherever its presence is unambiguously understood. Let us introduce the quasiparticle representation by

$$\begin{pmatrix} a^\dagger_{jm} \\ (-)^{j-m}a_{jm}\end{pmatrix}=\begin{pmatrix} u_j & -v_j \\ v_j & u_j\end{pmatrix}\begin{pmatrix} c^\dagger_{jm} \\ (-)^{j-m}c_{jm}\end{pmatrix}. \tag{2.2}$$

The phonon operator describing collective excitations in even-even nuclei within the QRPA is defined by using the following restricted representation

$$Q^\dagger_{a_2\alpha_2\mu_2}=\sum_{\tau=\pi,\nu}\sum_{j_1\leqslant j_2}[X_\tau(j_1j_2;a_2\alpha_2)\overline{A}^\dagger_{\alpha_2\mu_2}(j_1j_2) - Y_\tau(j_1j_2;a_2\alpha_2)(-)^{\alpha_2-\mu_2}\overline{A}_{\alpha_2-\mu_2}(j_1j_2)], \tag{2.3}$$

where we denote by $(a_2\alpha_2^p)$ the two-particle quantum numbers, namely, the energy eigenvalue, angular momentum and parity. For simplicity of notation, we drop the parity symbol whenever this is possible. The pair-creation operator is defined by the coupling of two particle-creation operators to some angular momentum,

$$A^\dagger_{\alpha_2\mu_2}(j_1j_2)=\sum_{m_1+m_2=\mu_2}\langle j_1m_1;j_2m_2|\alpha_2\mu_2\rangle a^\dagger_{j_1m_1}a^\dagger_{j_2m_2} \equiv(a^\dagger_{j_1}a^\dagger_{j_2})_{\alpha_2\mu_2}. \tag{2.4}$$

The normalized pair operator is given by

$$\overline{A}^\dagger_{\alpha_2\mu_2}(j_1j_2)=\frac{1}{\Delta_{j_1j_2}}A^\dagger_{\alpha_2\mu_2}(j_1j_2), \quad \Delta_{j_1j_2}\equiv\sqrt{1+\delta_{j_1j_2}(-)^{\alpha_2}}. \tag{2.5}$$

The boson commutation rules for the QRPA phonons, which constitute also our basis operators, lead to the usual orthonormality relations between the QRPA amplitudes. These relations allow us to invert Eq. (2.3) in a standard way. The QRPA equation of motion

$$[\hat{H},Q^\dagger_{a_2\alpha_2\mu_2}]=E_{a_2\alpha_2}Q^\dagger_{a_2\alpha_2\mu_2} \tag{2.6}$$

leads to the following matrix equation:

$$\begin{pmatrix} \mathcal{A} & \mathcal{B} \\ -\mathcal{B} & -\mathcal{A}\end{pmatrix}\begin{pmatrix} X_\tau \\ Y_\tau\end{pmatrix}=E_{a_2\alpha_2}\begin{pmatrix} X_\tau \\ Y_\tau\end{pmatrix}, \tag{2.7}$$

where the matrix elements are given in terms of symmetrized double commutators between the Hamiltonian and basis pair operators in Ref. [32]. The vacuum on which the matrix elements are estimated here is the Bardeen-Cooper-Schrieffer (BCS) state. Naturally, the $\mathcal{A}$ and $\mathcal{B}$ matrices contain the $\pi\pi\pi\pi$, $\pi\pi\nu\nu$, and $\nu\nu\nu\nu$ parts yielding to eigenvectors containing both the proton-proton and neutron-neutron two-quasiparticle amplitudes.

B. Two-phonon states

As we mentioned in the Introduction, the first example of a two-phonon state, investigated microscopically, was the low-lying 0^+ excitation in the Pb isotopes. The considered wave function was a product of the pairing pp and hh quadrupole excitations, i.e.,

$$\Gamma^\dagger_0=[Q^\dagger_2(pp)Q^\dagger_2(hh)]_0. \tag{2.8}$$

The resulting energy is just the sum of the positive pp and negative hh phonon energies. This is an example of a ''pure'' one-component two-phonon excitation. In describing low-lying excitations in even-even nuclei it is necessary to consider a more general superposition of one- and two-phonon components. Therefore, the resulting excitation operator can be defined as

$$\Gamma^{\dagger}_{a_4\alpha_4\mu_4}=\sum_{a_2} Z_1(a_2;a_4\alpha_4)Q^{\dagger}_{a_2\alpha_4\mu_4} + \sum_{a_2\alpha_2\leqslant b_2\beta_2} Z_2(a_2\alpha_2b_2\beta_2;a_4\beta_4) \times(Q^{\dagger}_{a_2\alpha_2}Q^{\dagger}_{b_2\beta_2})_{\alpha_4\mu_4}, \quad (2.9)$$

where $(a_4\alpha_4)$ denotes the eigenvalue index and total spin parity of the state. The energies associated with this excitation are, of course, not anymore sums of the single-phonon energies. The eigenstates can be found by using, for instance, the equation-of-motion technique, i.e.,

$$[\hat{H},\Gamma^{\dagger}_{a_4\alpha_4\mu_4}]=\mathcal{E}_{a_4\alpha_4}\Gamma^{\dagger}_{a_4\alpha_4\mu_4}. \quad (2.10)$$

To this purpose we proceed in a similar way we derived the QRPA equations. Namely, we compute the expectation value of the symmetrized double commutators between the Hamiltonian and the basis components entering Eq. (2.9) using the BCS vacuum. One gets the following system of equations:

$$\begin{pmatrix} E_{a_2\alpha_4}\delta_{a_2a_2'} & \mathcal{H}_{12}(a_2;a_2'\alpha_2'b_2'\beta_2') \\ \mathcal{H}_{21}(a_2\alpha_2b_2\beta_2;a_2') & \mathcal{H}_{22}(a_2\alpha_2b_2\beta_2;a_2'\alpha_2'b_2'\beta_2') \end{pmatrix} \times\begin{pmatrix} Z_1(a_2';a_4\alpha_4) \\ Z_2(a_2'\alpha_2'b_2'\beta_2';a_4\alpha_4) \end{pmatrix} = \mathcal{E}_{a_4\alpha_4}\begin{pmatrix} \delta_{a_2a_2'} & 0 \\ 0 & \mathcal{I}_{\alpha_4}(a_2\alpha_2b_2\beta_2;a_2'\alpha_2'b_2'\beta_2') \end{pmatrix} \times\begin{pmatrix} Z_1(a_2';a_4\alpha_4) \\ Z_2(a_2'\alpha_2'b_2'\beta_2';a_4\alpha_4) \end{pmatrix}. \quad (2.11)$$

Here the metric matrix is defined as

$$\mathcal{I}_{\alpha_4}(a_2\alpha_2b_2\beta_2;a_2'\alpha_2'b_2'\beta_2') =\langle 0|[(Q_{b_2\beta_2}Q_{a_2\alpha_2})_{\alpha_4},(Q^{\dagger}_{a_2'\alpha_2'}Q^{\dagger}_{b_2'\beta_2'})_{\alpha_4}]|0\rangle, \quad (2.12)$$

and its explicit form is derived in the Appendix. The Hamiltonian matrix elements are given in terms of symmetrized double commutators as follows:

$$\mathcal{H}_{22}(a_2\alpha_2b_2\beta_2;a_2'\alpha_2'b_2'\beta_2') =\langle 0|[(Q_{b_2\beta_2}Q_{a_2\alpha_2})_{\alpha_4},\hat{H},(Q^{\dagger}_{a_2'\alpha_2'}Q^{\dagger}_{b_2'\beta_2'})_{\alpha_4}]|0\rangle,$$

$$\mathcal{H}_{12}(a_2;a_2'\alpha_2'b_2'\beta_2')=\langle 0|[Q_{a_2\alpha_4},\hat{H},(Q^{\dagger}_{a_2'\alpha_2'}Q^{\dagger}_{b_2'\beta_2'})_{\alpha_4}]|0\rangle,$$

$$\mathcal{H}_{21}(a_2\alpha_2b_2\beta_2;a_2')=\langle 0|[(Q_{b_2\beta_2}Q_{a_2\alpha_2})_{\alpha_4},\hat{H},Q^{\dagger}_{a_2'\alpha_4}]|0\rangle. \quad (2.13)$$

By using the QRPA equation of motion (2.6) one finds that the elements $\mathcal{H}_{22}$ are proportional to the metric matrix, i.e.,

$$\mathcal{H}_{22}(a_2\alpha_2b_2\beta_2;a_2'\alpha_2'b_2'\beta_2') =\frac{1}{2}[E_{a_2\alpha_2}+E_{b_2\beta_2}+E_{a_2'\alpha_2'}+E_{b_2'\beta_2'}] \times\mathcal{I}_{\alpha_4}(a_2\alpha_2b_2\beta_2;a_2'\alpha_2'b_2'\beta_2'). \quad (2.14)$$

We stress here the fact that this form of the Hamiltonian matrix elements, connecting the two-phonon components, is simpler than in the standard MSM or QPM. It is similar to the already used TDA-level procedure of our earlier paper [16]. The matrix element $\mathcal{H}_{22}$ has a clear physical meaning, namely, it gives the main contribution to the two-phonon energies as a sum of energies of its one-phonon constituents, corrected by the Pauli principle (metric matrix).

In order to derive the matrix elements connecting one-phonon with two-phonon components, we consider the commutator of a QRPA phonon with the residual $H^{(31)}$ interaction. The result can be cast into a form written in terms of two QRPA phonons, i.e.,

$$[H^{(31)},Q^{\dagger}_{a_2\alpha_4\mu_4}] \rightarrow\sum_{d_2\gamma_2'c_2\gamma_2} C(d_2\gamma_2'c_2\gamma_2;a_2\alpha_4)(Q^{\dagger}_{d_2\gamma_2'}Q^{\dagger}_{c_2\gamma_2})_{\alpha_4\mu_4}, \quad (2.15)$$

where the coefficient C is given in the Appendix. In this way one obtains the following relations:

$$\mathcal{H}_{21}(a_2\alpha_2b_2\beta_2;a_2')=\frac{1}{2}\sum_{d_2\gamma_2'c_2\gamma_2} C(d_2\gamma_2'c_2\gamma_2;a_2'\alpha_4) \times\mathcal{I}_{\alpha_4}(a_2\alpha_2b_2\beta_2;d_2\gamma_2'c_2\gamma_2),$$

$$\mathcal{H}_{12}(a_2;a_2'\alpha_2'b_2'\beta_2')=\frac{1}{2}\sum_{d_2\gamma_2'c_2\gamma_2} C(d_2\gamma_2'c_2\gamma_2;a_2\alpha_4) \times\mathcal{I}_{\alpha_4}(d_2\gamma_2'c_2\gamma_2;a_2'\alpha_2'b_2'\beta_2') =\mathcal{H}_{21}(a_2'\alpha_2'b_2'\beta_2';a_2). \quad (2.16)$$

A similar procedure to estimate the coupling between the one- and two-phonon basis components is used in the QPM [17].

C. Electromagnetic transitions

The electromagnetic transitions between states containing only two-phonon components were described in Ref. [25]. Here we consider a more general case given by Eq. (2.9). The electromagnetic operator of multipolarity J is written in second quantization as follows:

$$T_{JM}=\sum_{\tau} e_{\tau}\sum_{ij}\langle\tau im_i|T_{JM}|\tau jm_j\rangle c^{\dagger}_{im_i}c_{jm_j} =\frac{1}{\hat{J}}\sum_{\tau} e_{\tau}\sum_{ij}\langle\tau i||T_J||\tau j\rangle[c^{\dagger}_i\tilde{c}_j]_{JM}, \quad (2.17)$$

where the transition operator for a harmonic-oscillator single-particle basis has the standard form

$$T_{JM}=r^J i^J Y_{JM}. \tag{2.18}$$

In the quasiparticle representation (2.2) the particle-hole part of the transition operator, consistent with the QRPA phonon (2.3), is given by

$$T_{JM}\rightarrow\sum_{\tau}\sum_{ij}\xi_{\tau J}(ij)[\overline{A}^{\dagger}_{JM}(ij)+(-)^{J-M}\overline{A}_{J-M}(ij)], \tag{2.19}$$

where

$$\xi_{\tau J}(i_\tau j_\tau)=\frac{e_\tau}{\hat{J}\Delta_{ij}}\langle\tau i||T_J||\tau j\rangle(u_i v_j+v_i u_j). \tag{2.20}$$

Here it is worth noting that we neglected the scattering terms $a^{\dagger}a$ because we will discuss only transitions between eigenstates with large one-phonon amplitudes and eigenstates with large two-phonon components. The reduced matrix element connecting an eigenstate with the ground state is given in terms of the one-phonon amplitudes of the operator (2.9), i.e.,

$$\begin{aligned}\langle a_4\alpha_4||T_{\alpha_4}||0\rangle&=\hat{\alpha}_4\sum_{a_2}Z_1(a_2;a_4\alpha_4)\sum_{\tau}\sum_{i\leqslant j}\xi_{\tau\alpha_4}(ij)[X_\tau(ij;a_2\alpha_4)\\&\quad+Y_\tau(ij;a_2\alpha_4)].\end{aligned} \tag{2.21}$$

The matrix element connecting two eigenstates is given as a superposition of components containing products between the one- and two-phonon amplitudes, multiplied by the metric matrix, i.e.,

$$\begin{aligned}\langle a_4'\alpha_4'||T_{\gamma_2}||a_4\alpha_4\rangle&=\sum_{\tau}\sum_{i\leqslant j}\sum_{c_2}\xi_{\tau\gamma_2}(ij)[X_\tau(ij;c_2\gamma_2)+Y_\tau(ij;c_2\gamma_2)]\\&\times\Bigg\{\hat{\alpha}_4'\sum_{a_2}\sum_{a_2'\alpha_2'\leqslant b_2'\beta_2'}Z_1(a_2;a_4\alpha_4)Z_2(a_2'\alpha_2'b_2'\beta_2';a_4'\alpha_4')\mathcal{I}_{\alpha_4'}(a_2'\alpha_2'b_2'\beta_2';a_2\alpha_4c_2\gamma_2)\\&+\hat{\alpha}_4\sum_{a_2'}\sum_{a_2\alpha_2\leqslant b_2\beta_2}Z_1(a_2';a_4'\alpha_4')Z_2(a_2\alpha_2b_2\beta_2;a_4\alpha_4)\mathcal{I}_{\alpha_4}(a_2'\alpha_4'c_2\gamma_2;a_2\alpha_2b_2\beta_2)\Bigg\}.\end{aligned} \tag{2.22}$$

In conclusion, the metric matrix, taking into consideration the Pauli principle, is the most important ingredient in our approach describing both eigenstates and electromagnetic transitions.

D. Two-level model

To get a rough idea about the ingredients of the present formalism, let us first consider an application to a two-level model. Now the basic building block of the two-phonon state is simply a quadrupole QRPA phonon, and the excitations are superpositions of one- and two-phonon components in the form

$$\Gamma^{\dagger}_J=Z_1(J)Q^{\dagger}_J+Z_2(J)(Q^{\dagger}_2Q^{\dagger}_2)_J,\quad J=0,2,4. \tag{2.23}$$

For simplicity, we consider that the monopole one-phonon component, corresponding to the breathing mode, vanishes, i.e., $Z_1(0)=0$. The system of equations for two-phonon states (2.11) becomes

$$\begin{pmatrix}E_J & \mathcal{H}_J\\ \mathcal{H}_J & 2E_2\mathcal{I}_J\end{pmatrix}\begin{pmatrix}Z_1(J)\\ Z_2(J)\end{pmatrix}=\mathcal{E}_J\begin{pmatrix}1 & 0\\ 0 & \mathcal{I}_J\end{pmatrix}\begin{pmatrix}Z_1(J)\\ Z_2(J)\end{pmatrix},\quad J=0,2,4, \tag{2.24}$$

where $E_0=0$, and E_2,E_4 are the lowest QRPA eigenvalues, $\mathcal{I}_J$ the metric two-phonon matrix elements, and $\mathcal{H}_J$ the interaction term between the one- and two-phonon components. The solutions corresponding to $\mathcal{E}^{(2)}_2$ and $\mathcal{E}^{(1)}_4$ have large two-phonon components $Z_2(J)$. It is interesting to note that the following inequality holds:

$$\begin{aligned}\frac{\mathcal{E}^{(1)}_4-\mathcal{E}^{(2)}_2}{E_2}&=\frac{E_4}{2E_2}-1-\sqrt{\left(\frac{E_4}{2E_2}-1\right)^2+\frac{\mathcal{H}_4^2}{\mathcal{I}_4E_2^2}}+\frac{1}{2}\\&\quad-\sqrt{\frac{1}{4}+\frac{\mathcal{H}_2^2}{\mathcal{I}_2E_2^2}}\leqslant 0,\end{aligned} \tag{2.25}$$

because the left-hand side is a sum of two negative quantities. Therefore, the energy of the 4^+_1 state, being of the two-phonon character, is always lower that the energy of the 2^+_2 two-phonon-like state. If the coupling between the one- and two-phonon components, namely, $\mathcal{H}_J$, is small, one obtains the well known near-degenerate triplet of two-phonon states $0^+_2,2^+_2,4^+_1$ (we label the ground state by 0^+_1). In the absence of coupling one obtains a degenerate triplet. It is also interesting to discuss the $B(E2)$ values, defined as

TABLE I. Experimental energies in keV for ^{106}Pd [34] (second column), energies of the two-level model (third column), and the components of the wave function (last two columns).

J_l^π	$E_{\rm exp}$	$E_{\rm th}$	$Z_1(J_1^+)$	$Z_2(2_1^+2_1^+)_J$
4_2^+	1932	2262	0.989	0.111
4_1^+	1229	1165	−0.151	0.728
0_2^+	1134	1190		0.749
2_2^+	1128	1286	−0.349	0.682
2_1^+	512	500	0.939	0.254

$$B(E2;J_i\rightarrow J_f)=\left[\frac{\langle J_f\|T_2\|J_i\rangle}{\hat{J}_i}\right]^2, \tag{2.26}$$

within this simple model. One can directly use Eqs. (2.21) and (2.22) to obtain the following branching ratio:

$$R_J=\frac{B(E2;J^+\rightarrow 2_1^+)}{B(E2;2_1^+\rightarrow 0_1^+)}=[Z_2(J)\mathcal{I}_J]^2, \quad J^+=0_2^+,2_2^+,4_1^+ . \tag{2.27}$$

If one considers boson commutation rules, i.e., $\mathcal{I}_J=2$ and $Z_2(J)=1/\sqrt{2}$, then one obtains for the above ratio the value 2.

III. NUMERICAL APPLICATION

A systematic analysis showed that the Ru-Pd region [33,34] and Cd isotopes [35,36] contain many examples of multiphonon structures. Probably the best, almost degenerate, two-phonon triplet of states $0^+,2^+,4^+$ is seen in ^{106,108}Pd [34]. Our interest in studying the Pd isotopes is also connected with the possible beta and double-beta transitions to this triplet of states. Many papers were devoted to the theoretical analysis of the Pd isotopes [37–43], most of them at a phenomenological level.

An important ingredient of our microscopic approach is the single-particle basis. We describe it by using eigenvalues of the spherical Woods-Saxon nuclear mean field. The single-particle wave functions are taken, however, to be eigenstates of a spherical harmonic-oscillator with a suitable oscillator constant. This is a rather good approximation for bound states in the Pd isotopes. We have chosen for the ^{106,108}Pd isotopes 12 proton and 15 neutron single-particle levels around the Fermi surface. Some of the Woods-Saxon energies have been shifted slightly to better reproduce the low-energy one-quasiparticle-like spectra of the neighboring proton- and neuton-odd nuclei. The same single-particle valence space was recently used for the study of the beta- and double-beta decay feeding of ^{106}Pd in Ref. [44]. The BCS occupation amplitudes and the QRPA eigenstates were calculated using as a residual two-body interaction the *G*-matrix elements of the Bonn one-boson-exchange interaction, as done in Ref. [44]. Different channels of this interaction were scaled by a constant as described in Ref. [44].

TABLE II. Experimental ratios $R(E2)$ between $B(E2)$ values and $B(E2;2_1^+\rightarrow 0_1^+)$ for ^{106}Pd [34] (second column) and the $R(E2)$ values of the two-level model (third column).

$J_i\rightarrow J_f$	$R(E2)_{\rm exp}$	$R(E2)_{\rm th}$
$0_2^+\rightarrow 2_1^+$	1.02	1.78
$2_2^+\rightarrow 2_1^+$	0.93	1.23
$4_2^+\rightarrow 2_1^+$	1.69	1.80
$2_2^+\rightarrow 0_1^+$	0.02	0.14

TABLE III. Experimental energies in keV for ^{106}Pd [34] (second column), the QRPA energies (third column), and calculated energies for different numbers of the QRPA 2^+ and 4^+ eigenstates.

J_l^π	$E_{\rm exp}$	$E_{\rm QRPA}$	$E_{N=1}$	$E_{N=2}$	$E_{N=3}$	$E_{N=4}$	$E_{N=5}$
4_2^+	1932	2246	2183	2103	2087	2123	2093
0_3^+	1707		4493	2874	2752	3136	3103
2_3^+	1562	2245	2935	2104	1998	1977	1975
4_1^+	1229		1281	1240	1166	1193	1178
0_2^+	1134		1323	1301	1223	1294	1293
2_2^+	1128		1399	1367	1375	1323	1359
2_1^+	512	662	556	535	496	483	489

As a first application we considered the two-level wave function (2.23). The energies of the eigenstates $0_2^+,2_k^+,4_k^+$, $k=1,2$ for ^{106}Pd are given in the third column of Table I. In the last columns we give the components of their wave functions. We notice that the members of the triplet $0_2^+,2_2^+,4_1^+$ have a large two-phonon amplitude. We stress the fact that the two-phonon triplet is split and its centroid is pushed higher than twice the energy of the 2_1^+ state, in agreement with the experimental situation. We remind that this happens mainly because of the interaction between the one- and two-phonon components of the Hilbert space of the model and, to some extent, because of the *J* dependence of the metric matrix. One can see that the agreement of the predicted energies with the energies of the experimental levels, given in the second column, is within 200 keV.

In the last column of Table II we give the predicted ratios of the $B(E2)$ values to the quantity $B(E2;2_1^+\rightarrow 0_1^+)$. The predicted ratios from the members of the two-phonon triplet are less than the values predicted by the extreme boson limit due to the Pauli effect, accounted for by the metric matrix. Except for the first line of Table II, the agreement with the experimental values, given in the second column, is quite satisfactory.

For the general wave function (2.9) we solve the eigen-

TABLE IV. Experimental ratios $R(E2)$ between $B(E2)$ values and $B(E2;2_1^+\rightarrow 0_1^+)$ for ^{106}Pd [34] (second column) and calculated ratios for $N=5$ (third column).

$J_i\rightarrow J_f$	$R(E2)_{\rm exp}$	$R(E2)_{\rm th}$
$0_2^+\rightarrow 2_1^+$	1.02	1.87
$2_2^+\rightarrow 2_1^+$	0.93	1.55
$4_2^+\rightarrow 2_1^+$	1.69	1.77
$2_2^+\rightarrow 0_1^+$	0.02	0.13

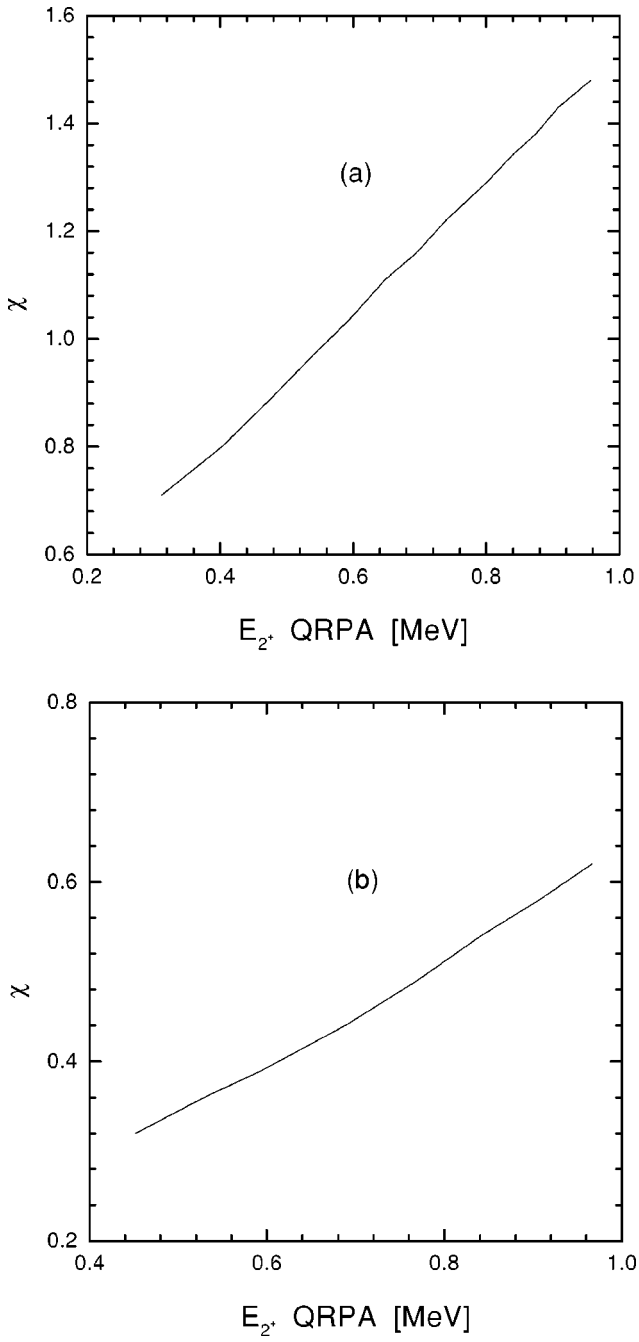

FIG. 1. (a) The effective charge parameter χ versus the energy of the first QRPA 2_1^+ phonon for the small single-particle basis with $N=5$. (b) The same as in (a), but for the large single-particle basis.

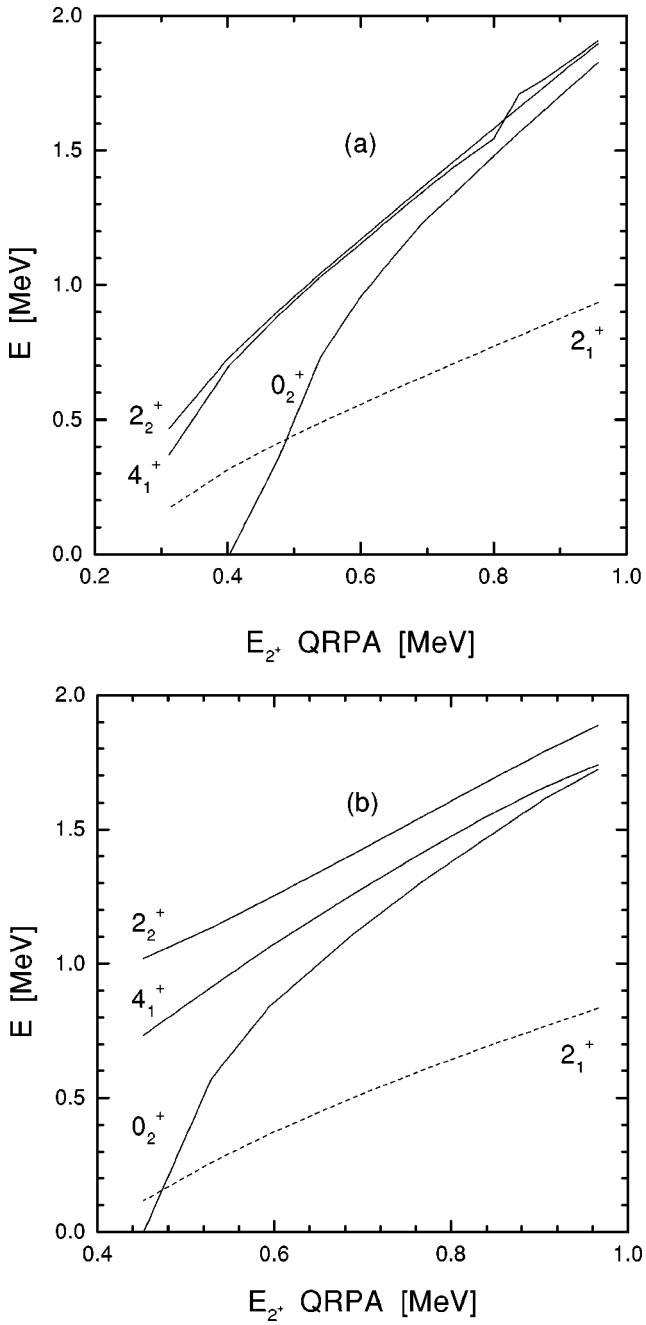

FIG. 2. (a) The lowest eigenvalues of the system (2.11) versus the energy of the first QRPA 2_1^+ phonon for the small single-particle basis with $N=5$. The lowest two-quasiparticle configuration in the 2_1^+ state of the QRPA calculation is $(\nu 1d_{5/2})^2$ with an energy of 2.01 MeV. (b) The same as in (a), but for the large single-particle basis and with the $(\nu 1d_{5/2})^2$ configuration energy of 2.73 MeV.

value system of equations (2.11) by using a standard technique [16]. The initial basis is not orthogonal and therefore the metric matrix is nondiagonal. First we diagonalize the metric matrix. The eigenstates of the metric matrix allow us to built a new orthonormal basis. The states corresponding to very small eigenvalues of the metric matrix are spurious and should be eliminated. The resulting system of equations in the new basis has a standard Hermitian form.

We build the two-phonon basis by using a given amount N of 2^+ and 4^+ QRPA eigenstates. The result of calculation for $N=1,\ldots,5$ in ^{106}Pd is given in Table III. We mention that after $N=5$, convergence in the energies of the low-lying states is achieved. In the third column we give the starting QRPA eigenvalues for those states with a large one-phonon component. The agreement with the experimental spectrum of the second column is within 200 keV, except for the eigenstate 0_3^+. The accuracy for the two-phonon-like triplet is comparable with the result of the two-level model but, of course, here a host of other levels are described.

To have a feel of the systematic behavior of our model,

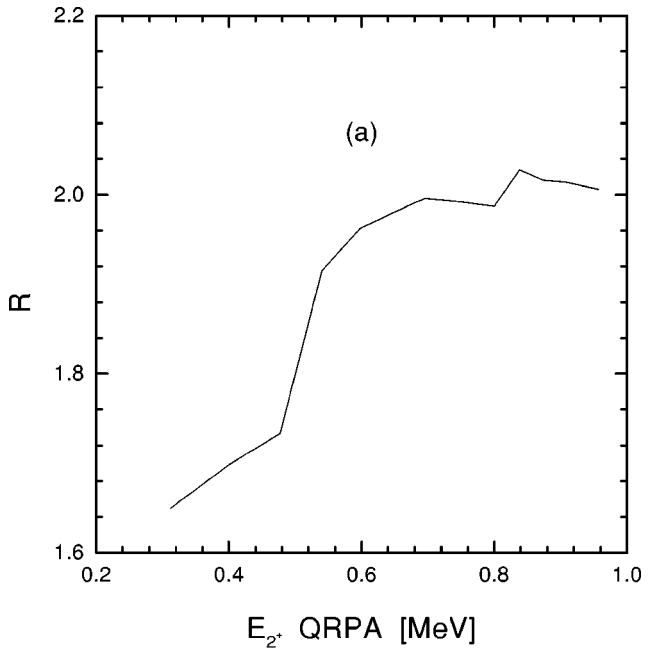

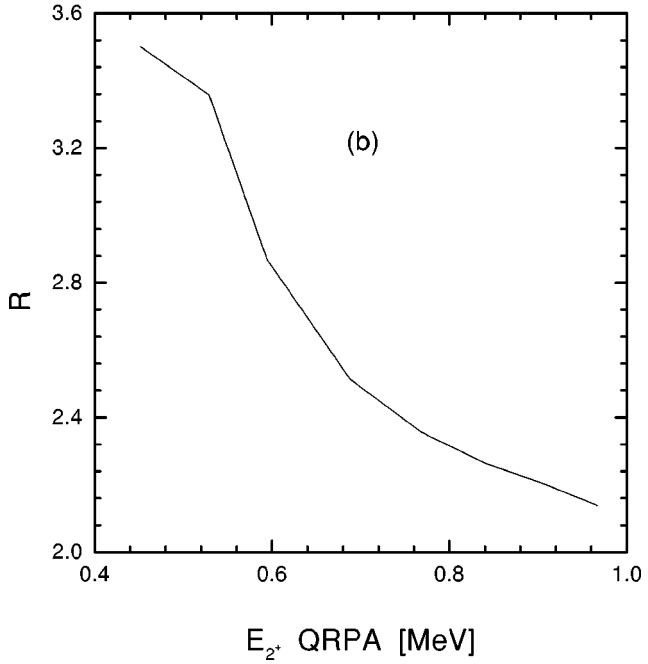

FIG. 3. (a) The ratio between the energies of the triplet centroid and the eigenvalue 2_1^+ versus the energy of the first QRPA 2_1^+ phonon for the small single-particle basis with $N=5$. (b) The same as in (a), but for the large single-particle basis.

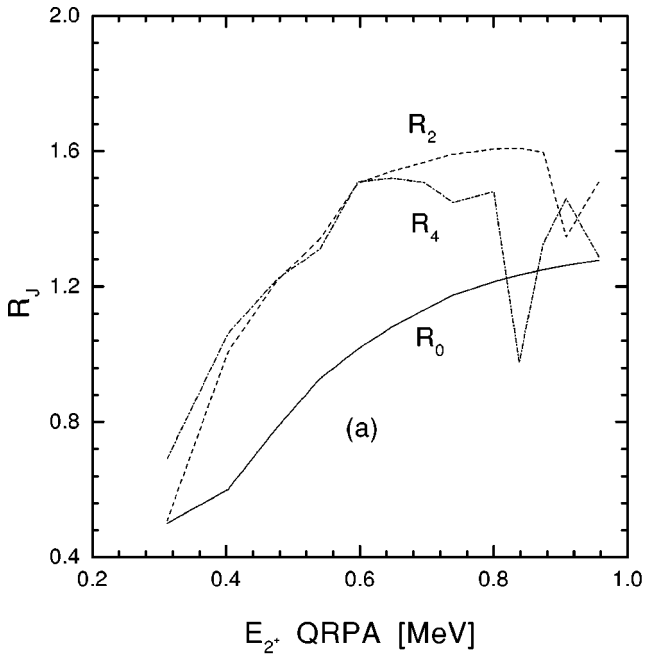

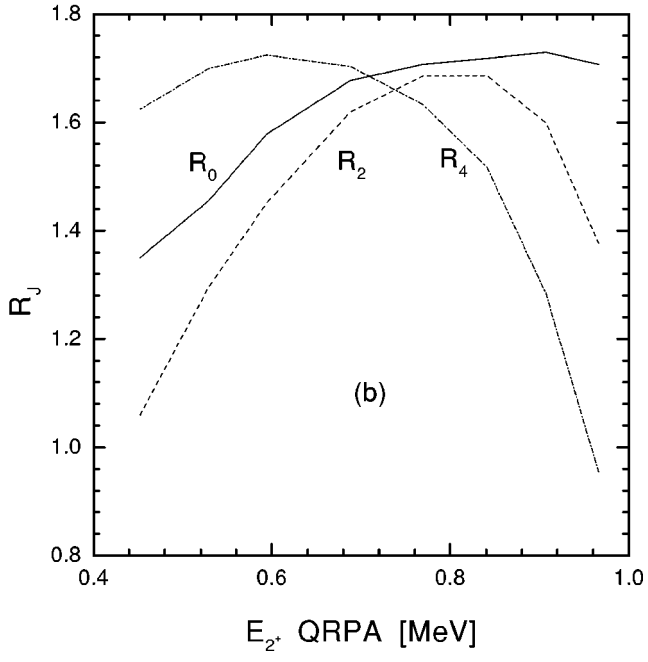

FIG. 4. (a) The ratios R_J defined by Eq. (2.27) versus the energy of the first QRPA 2_1^+ phonon for the small single-particle basis with $N=5$. (b) The same as in (a), but for the large single-particle basis.

we discuss next the ^{106}Pd nucleus in terms of two basis sets. The first is a *small* (toy) basis set consisting of three proton and neutron orbitals in the immediate vicinity of the corresponding Fermi surfaces. The second is the one mentioned previously (12 proton and 15 neutron single-particle states), which we call here the *large* basis set. The collectivity of the lowest 2^+ state can be seen both from its energy and its electric quadrupole decay strength to the 0_1^+ ground state. For ^{106}Pd the measured reduced quadrupole transition probability from the 2_1^+ state to the ground state is $B(E2)_{\rm exp}=42\pm4$ W.u. [34]. The corresponding theoretical $B(E2)$ can be brought to this value by defining the effective proton and neutron charges using the effective-charge polarization parameter χ [45]. In Fig. 1 we display values of this parameter as a function of the energy of the lowest 2^+ state of the QRPA calculation. Here Fig. 1(a) concerns the small basis and Fig. 1(b) the large basis. As can be seen from these figures, the collectivity of the 2_1^+ state increases when its energy decreases, thus needing smaller and smaller effective charges to reproduce the experimental $B(E2)$. For the small basis the lowest two-quasiparticle energy is at around 2 MeV

TABLE V. Experimental energies in keV for ^{108}Pd [34] (second column), the QRPA energies (third column), and calculated energies for different numbers of the QRPA 2^+ and 4^+ eigenstates.

J_l^π	$E_{\rm exp}$	$E_{\rm QRPA}$	$E_{N=1}$	$E_{N=2}$	$E_{N=3}$	$E_{N=4}$	$E_{N=5}$
4_2^+	1624	2179	2114	2024	2016	1996	1987
0_3^+	1314		4358	2859	2819	3061	3066
2_3^+	1441	2245	2837	2061	2051	1923	1916
4_1^+	1048		1230	1164	1112	1087	1099
0_2^+	1053		1274	1235	1188	1296	1289
2_2^+	931		1367	1317	1306	1299	1305
2_1^+	434	637	519	470	468	407	400

and for the large basis at around 2.7 MeV (the more exact values are given in the caption of Fig. 2). It is also evident from Fig. 1 that for the small basis one needs bigger effective charges than for the large basis.

In Fig. 2 we show the energies of the 2_1^+ state and the two-phonon triplet as functions of the energy of the first 2^+ phonon of the QRPA. Both for the small basis [Fig. 2(a)] and the large basis [Fig. 2(b)] the energies of these states are very little perturbed for the QRPA 2^+ energies close to 1 MeV (energies to the very right in Fig. 2). As the energy of the QRPA 2^+ state decreases, and thus its collectivity increases, the two-phonon triplet splits more and more in energy and the energy of the 2_1^+ state goes faster to zero than the QRPA 2^+ phonon energy. As a matter of fact, the first two-phonon 0^+ state collapses for very small values of the QRPA 2^+ energy. One can also see that the splitting of the triplet is more notable for the large basis. The development of the relative energies of the 2_1^+ and the two-phonon states is shown in Fig. 3 where (a) shows the ratio R between the centroid energy of the two-phonon triplet and the energy of the 2_1^+ state as a function of the QRPA 2^+ energy for the small basis. Figure 3(b) shows the same for the large basis. As seen from this figure the behavior of this ratio is qualitatively very different for the small and large bases: for the small basis R decreases and for the large basis it increases with decreasing energy (increasing collectivity) of the QRPA 2^+ state. The behavior of R in the large basis is along the lines of experiment where for ^{106}Pd $R_{\rm exp}=2.27$.

In Fig. 4 we show the ratios R_J of Eq. (2.27) for the small basis [Fig. 4(a)] and the large basis [Fig. 4(b)] as functions of the QRPA 2^+ phonon energy. For the small basis the behavior as a function of the QRPA 2^+ energy is more monotonous than for the large basis where all the ratios R_J have a maximum at some value of the 2^+ energy. The abrupt changes in the ratios R_2 and R_4 for the small basis and large 2^+ energy come from the strong mixing of the one-phonon states with these two-phonon states at large energies of the two-phonon triplet. It is worth noting that for the large basis the ratios tend towards their experimental values, displayed in Table IV, with the decreasing energy of the QRPA 2^+ phonon.

In Fig. 5(a) we display eigenvalues of the metric matrix for the $J=0$ (squares), $J=2$ (stars), and $J=4$ (triangles) states in the case of the large basis, for $N=5$ and at a realistic value of the energy of the QRPA 2^+ phonon. For the states of the two-phonon triplet the diagonal matrix elements of the metric matrix are between 1.84 and 1.93 and the off-diagonal elements below 0.12. In Fig. 5(b) we display the magnitudes of the Hamiltonian matrix elements for the $J=2$ states for the above mentioned large basis and the realistic QRPA 2^+ energy. Here the squares are the diagonal matrix elements and the circles are the maximum values of the nondiagonal elements. As can be seen, the magnitudes of the off-diagonal elements are typically of the order of 0.2–0.3 MeV, much smaller than the diagonal ones, of the order of 3 MeV. In particular, for the two-phonon triplet states the diagonal elements are between 2.53–2.57 MeV and the magnitudes of the matrix elements connecting them to the 2_1^+ and 4_1^+ one-phonon states between 0.2 and 0.3 MeV.

The behaviors of the metric matrix elements and Hamiltonian matrix elements related to the two-phonon triplet have been displayed in Fig. 6 as functions of the energy of the 2_1^+ phonon of the QRPA. The calculation has been performed for the large basis with $N=5$. The displayed diagonal metric matrix elements for the two-phonon triplet [Fig. 6(a)] decrease slowly with the increasing collectivity of the 2_1^+ state. At the same time, the corresponding diagonal Hamiltonian matrix elements [Fig. 6(b)] decrease fast to less than half of their initial value and the nondiagonal matrix elements connecting the 2_1^+ and 4_1^+ states with the $2_{2\text{-}ph}^+$ and $4_{2\text{-}ph}^+$ states, respectively, increase their magnitude [Fig. 6(b)]. This means that the repulsion between these one- and two-phonon states increases considerably with increasing collectivity of the 2_1^+ state leading to a very low final energy for the 2_1^+ state. In addition, the strongest off-diagonal matrix elements in $\mathcal{H}_{12}$ of Eq. (2.11) are the ones of $J=0$ angular momentum lead-

TABLE VI. Largest components of the wave functions for ^{106}Pd with $N=5$.

J_l^π	$Z_1(J_1^+)$	$Z_1(J_2^+)$	$Z_2(2_1^+2_1^+)_J$	$Z_2(2_1^+2_2^+)_J$	$Z_2(2_1^+2_3^+)_J$	$Z_2(2_1^+4_1^+)_J$
4_2^+	0.851		0.143	−0.371		0.339
0_3^+				−0.781	0.840	
2_3^+	−0.119	0.869	−0.122	0.268	0.269	−0.197
4_1^+	−0.184		0.753	0.248		
0_2^+			0.752			
2_2^+	−0.304	0.154	0.679			
2_1^+	0.933		0.213			

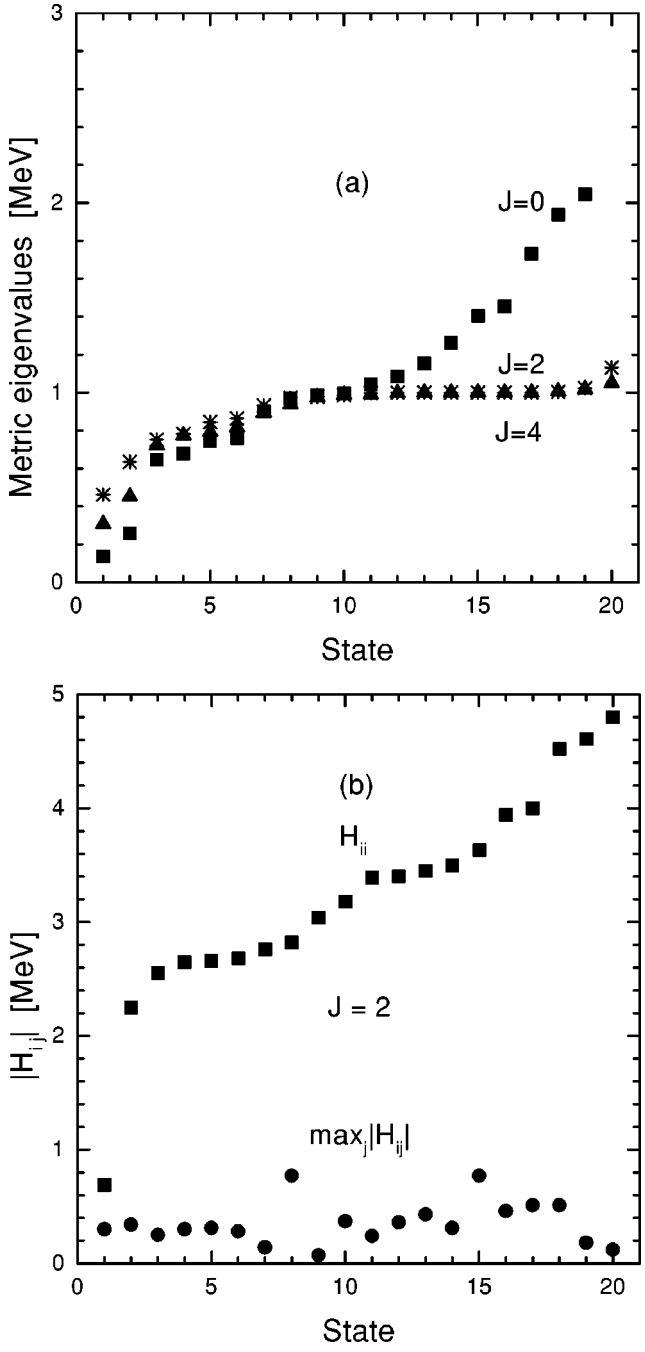

FIG. 5. (a) Eigenvalues of the metric matrix for the large single-particle basis with $N=5$. A realistic value of the 2_1^+ state was used. The squares, stars, and triangles correspond to $J=0$, $J=2$, and $J=4$ states, respectively. (b) The same as in (a), but for the magnitudes of the Hamiltonian matrix elements [for the Hamiltonian $\mathcal{H}_{12}$ of Eq. (2.11)] in the case of $J=2$. The squares denote the magnitudes of the diagonal matrix elements and the circles the maximum magnitudes of the off-diagonal elements.

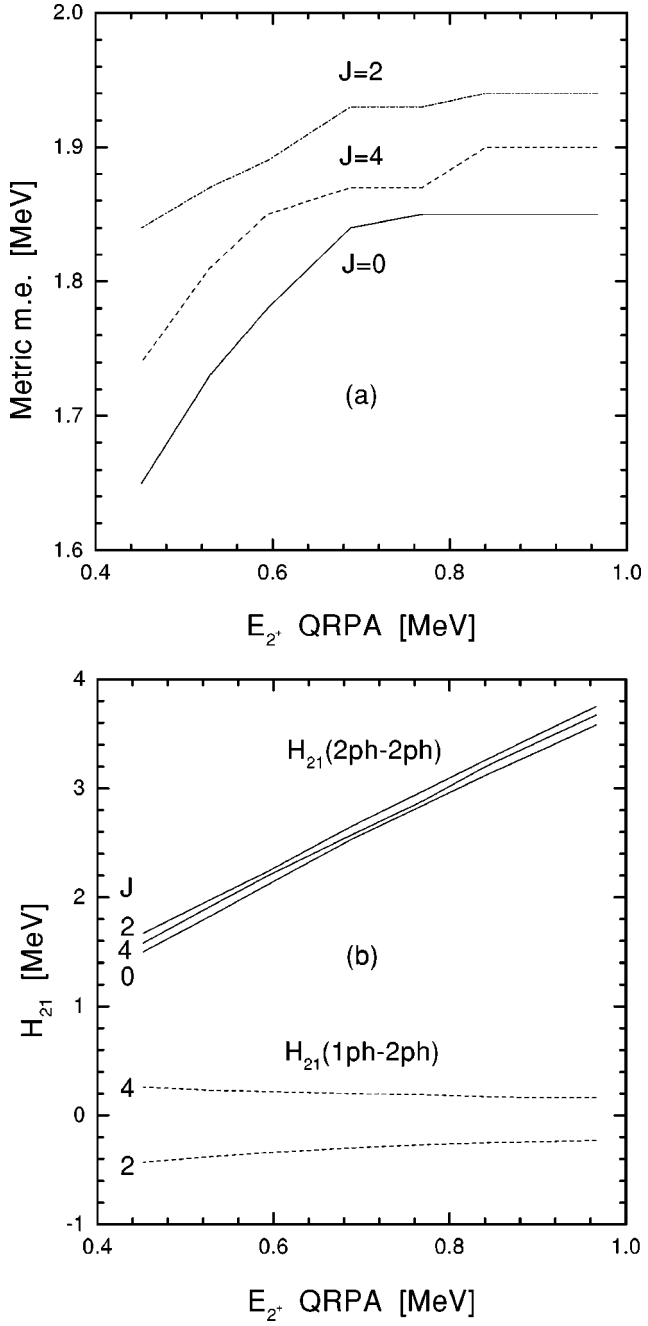

FIG. 6. (a) Values of the metric matrix elements for the two-phonon states as functions of the energy of the first QRPA 2_1^+ phonon. (b) Values of the Hamiltonian $\mathcal{H}_{12}$ matrix elements for the two-phonon states as functions of the energy of the first QRPA 2_1^+ phonon. The interaction matrix elements of the two-phonon states with the first one-phonon state of the same angular momentum are also given.

ing to the collapse of the 0^+ two-phonon state before the collapse of the 2_1^+ state, as clearly seen in Fig. 2.

The convergence of the energy spectrum of ^{108}Pd is shown in Table V. As for ^{106}Pd, convergence is achieved for $N=5$. To have a deeper insight into the contents of the wave functions, we give in Table VI the main components of the wave functions of states in ^{106}Pd. The members of the triplet $0_2^+,2_2^+,4_1^+$ have a large $(2_1^+2_1^+)_J$ component, comparable to that of the two-level case. The eigenstate 0_3^+ has large two-phonon components $(2_1^+2_2^+)_0$ and $(2_1^+2_3^+)_0$. The corresponding results for ^{108}Pd are given in Table VII.

The ratios of the $B(E2)$ values are described in Table IV for ^{106}Pd and in Table VIII for ^{108}Pd. We used in the calculations the effective-charge polarization parameter $\chi=0.4$ for

TABLE VII. Largest components of the wave functions for ^{108}Pd with $N=5$.

J_l^π	$Z_1(J_1^+)$	$Z_1(J_2^+)$	$Z_2(2_1^+2_1^+)_J$	$Z_2(2_1^+2_2^+)_J$	$Z_2(2_1^+2_3^+)_J$	$Z_2(2_1^+4_1^+)_J$
4_2^+	0.836	−0.179	0.151	−0.322	−+0.101	0.344
0_3^+				−0.519	1.019	
2_3^+	−0.167	0.838	−0.121	0.285		−0.172
4_1^+	−0.185		0.761	0.283	0.119	−0.106
0_2^+			0.752	−0.156	−0.150	
2_2^+	−0.315	0.151	0.678			
2_1^+	0.918	0.118	0.222	0.133		−0.102

^{106}Pd and $\chi=0.5$ for ^{108}Pd in order to reproduce the absolute value of the $B(E2;2_1^+\rightarrow 0^+)$. One can see that, except the first transition, these ratios satisfactorily describe the experimental situation.

IV. CONCLUSIONS

In this paper we derived a simple formalism to describe two-phonon-like excitations in even-even nuclei. The procedure has two steps. First we determined the QRPA phonons using single-particle energies of a spherical Woods-Saxon mean field plus a residual interaction, calculated within the *G*-matrix approach. The two-phonon-like excitations were built as superpositions of one- and two-phonon components with a given angular momentum and parity. The equations of motion for these states were derived using the QRPA equations from the previous step. It turned out that the Hamiltonian matrix elements connecting the two-phonon components are proportional to the metric matrix. The connection between the one- and two-phonon components is given by the $H^{(31)}$ part of the residual Hamiltonian in its quasiparticle representation. Electromagnetic transitions between the two-phonon states are described in terms of the same metric matrix.

Our calculation gives an energy-split triplet of low-lying 0^+, 2^+, 4^+ states, due to interaction between the one- and two-phonon components. Analysis of the amplitude content showed that, indeed, these states have a two-phonon nature. The centroid of the tripled is pushed up, in agreement with the experimental situation. The experimental energy levels and $B(E2)$ values are quite well reproduced, except the energy of the 0_3^+ state and the transition from the 0_2^+ state. The energy of the 4^+ two-phonon-like state is lower than the energy of the 2^+ two-phonon-like state, as predicted by the two-level model, in contrast to the experiment. We think that these drawbacks are connected with the fact that the considered Pd isotopes have a moderate quadrupole deformation. Therefore, proper description of a deformed system would be necessary to reproduce the very fine details of the orderings of the triplet of the two-phonon-like states.

TABLE VIII. Experimental ratios $R(E2)$ between $B(E2)$ values and $B(E2;2_1^+\rightarrow 0_1^+)$ for ^{108}Pd [34] (second column) and calculated ratios for $N=5$ (third column).

$J_i\rightarrow J_f$	$R(E2)_{\rm exp}$	$R(E2)_{\rm th}$
$0_2^+\rightarrow 2_1^+$	1.04	1.93
$2_2^+\rightarrow 2_1^+$	1.02	1.42
$4_2^+\rightarrow 2_1^+$	1.48	1.77
$2_2^+\rightarrow 0_1^+$	0.01	0.15

ACKNOWLEDGMENTS

One of us (D.S.D.) expresses his thanks for the hospitality of the Department of Physics of the University of Jyväskylä during his stay in Jyväskylä, where this work was performed. This work was supported by the Academy of Finland under the Finnish Center of Excellence Program 2000-2005 (Project No. 44875, Nuclear and Condensed Matter Program at JYFL).

APPENDIX

In the following we use the exact commutators between two QRPA phonons:

$$
\begin{aligned}
&[Q_{a\alpha\mu},Q^\dagger_{a'\alpha'\mu'}]\\
&\quad=\delta_{aa'}\delta_{\alpha\alpha'}\delta_{\mu\mu'}+\sum_{j_1j_2j_1'}\sum_{m_1m_2m_1'}a^\dagger_{j_1'm_1'}a_{j_2m_2}\\
&\qquad\times\{\overline{X}_\tau(j_1j_2;a\alpha)\overline{X}_\tau(j_1'j_1;a'\alpha')\langle j_1m_1;j_2m_2|\alpha\mu\rangle\\
&\qquad\times\langle j_1'm_1';j_1m_1|\alpha\mu\rangle-\overline{Y}_\tau(j_1j_2;a\alpha)\overline{Y}_\tau(j_1'j_1;a'\alpha')\\
&\qquad\times\langle j_1m_1;j_2m_2|\alpha-\mu\rangle\langle j_1'm_1';j_1m_1|\alpha-\mu\rangle\\
&\qquad\times(-)^{\alpha+\alpha'-\mu-\mu'}\},
\end{aligned}
\tag{A1}
$$

in order to derive an expression of the metric matrix. The new amplitudes are defined in terms of the amplitudes of the restricted basis as follows:

$$
\begin{aligned}
&\overline{X}_\tau(j_1j_2;a_2\alpha_2)\\
&\quad=\begin{cases}X_\tau(j_1j_2;a_2\alpha_2)\Delta_{j_1j_2}, & j_1\leqslant j_2\\ X_\tau(j_2j_1;a_2\alpha_2)\Delta_{j_2j_1}(-)^{j_1+j_2-\alpha_2+1}, & j_1>j_2.\end{cases}
\end{aligned}
\tag{A2}
$$

To this purpose we use the unrestricted representation of the QRPA phonon. The result contains, in addition to the diagonal terms, a correction expressing the Pauli principle, i.e.,

$$\mathcal{I}_{\alpha_4}(a_2\alpha_2 b_2\beta_2; a_2'\alpha_2' b_2'\beta_2')$$
$$= \langle [(Q_{b_2\beta_2} Q_{a_2\alpha_2})_{\alpha_4}, (Q^\dagger_{a_2'\alpha_2'} Q^\dagger_{b_2'\beta_2'})_{\alpha_4}] \rangle$$
$$= \delta_{a_2 a_2'}\delta_{\alpha_2\alpha_2'}\delta_{b_2 b_2'}\delta_{\beta_2\beta_2'} + \delta_{a_2 b_2'}\delta_{\alpha_2\beta_2'}\delta_{b_2 a_2'}\delta_{\beta_2\alpha_2'}(-)^{\alpha_2+\beta_2-\alpha_4} - \sum_\tau \sum_{ijkl} A_\tau(ijkl; a_2\alpha_2 b_2\beta_2; a_2'\alpha_2' b_2'\beta_2'), \quad \text{(A3)}$$

where the above matrix A_τ is given by

$$A_\tau(ijkl; a_2\alpha_2 b_2\beta_2; a_2'\alpha_2' b_2'\beta_2')$$
$$= \hat{\alpha}_2\hat{\beta}_2\hat{\alpha}_2'\hat{\beta}_2' \begin{Bmatrix} i & j & \alpha_2 \\ k & l & \beta_2 \\ \alpha_2' & \beta_2' & \alpha_4 \end{Bmatrix} \times \{ \overline{X}_\tau(ij; a_2\alpha_2)\overline{X}_\tau(kl; b_2\beta_2) \times \overline{X}_\tau(ik; a_2'\alpha_2')\overline{X}_\tau(jl; b_2'\beta_2') - \overline{Y}_\tau(ij; a_2\alpha_2) \times \overline{Y}_\tau(kl; b_2\beta_2)\overline{Y}_\tau(ik; a_2'\alpha_2')\overline{Y}_\tau(jl; b_2'\beta_2') \}. \quad \text{(A4)}$$

The second term containing the product of four Y amplitudes is very small and can be safely neglected. In this way the metric matrix has a TDA form used in Ref. [16].

The residual interaction, connecting the one-phonon with the two-phonon components, has the following form in the quasiparticle representation:

$$H_1^{(31)} = \sum_{\lambda_2\mu_2} \sum_\tau \sum_{ijkl} V_{ijkl}^{(31)}(\tau\lambda_2)(-)^{\lambda_2-\mu_2} \times [(a_i^\dagger a_j^\dagger)_{\lambda_2\mu_2}(a_k^\dagger \tilde{a}_l)_{\lambda_2-\mu_2} + \text{H.c.}]. \quad \text{(A5)}$$

Here we have dropped the isospin indices except under the summation sign.

The commutator giving two phonon-creation operators is given by

$$[H_1^{(31)}, Q^\dagger_{a_2\alpha_4\mu_4}] \to \sum_{d_2\gamma_2' c_2\gamma_2} C(d_2\gamma_2' c_2\gamma_2; a_2\alpha_4)(Q^\dagger_{d_2\gamma_2'} Q^\dagger_{c_2\gamma_2})_{\alpha_4\mu_4}, \quad \text{(A6)}$$

where the coefficient can be found by a straightforward calculation to be as follows:

$$C(d_2\gamma_2' c_2\gamma_2; a_2\alpha_4) = \sum_{\lambda_2} \sum_\tau \sum_{ijkl} V_{ijkl}^{(31)}(\tau\lambda_2) \sum_{m\leqslant n} \frac{X_\tau(mn; a_2\alpha_4)}{\Delta_{mn}} \{ \delta_{\gamma_2'\lambda_2}\hat{\lambda}_2\hat{\gamma}_2 [\overline{X}_\tau(ij; d_2\lambda_2)[x_\tau(\lambda_2 k\alpha_4 n; m\gamma_2; c_2)\delta_{lm} - (-)^{m+l-\alpha_4} x_\tau(\lambda_2 k\alpha_4 m; n\gamma_2; c_2)\delta_{ln}] + (-)^{l-k+\lambda_2}\overline{Y}_\tau(ij; d_2\lambda_2)[x_\tau(\lambda_2 l\alpha_4 n; m\gamma_2; c_2)\delta_{km} - (-)^{m+k-\alpha_4} x_\tau(\lambda_2 l\alpha_4 m; n\gamma_2; c_2)\delta_{kn}]] + \hat{\lambda}_2^2\hat{\gamma}_2\hat{\gamma}_2'(-)^{\gamma_2'}[(-)^{j+k} y_\tau(lkij; \lambda_2\gamma_2; c_2) \times [(-)^{i+m} x_\tau(\gamma_2 l\alpha_4 m; n\gamma_2'; d_2)\delta_{in} - (-)^{\alpha_4} x_\tau(\gamma_2 l\alpha_4 n; m\gamma_2'; d_2)\delta_{im}] - (-)^{\lambda_2-\alpha_4} y_\tau(lkji; \lambda_2\gamma_2; c_2) \times [(-)^{k+m} x_\tau(\gamma_2 l\alpha_4 m; n\gamma_2'; d_2)\delta_{jn} + (-)^{j+k} x_\tau(\gamma_2 l\alpha_4 n; m\gamma_2'; d_2)\delta_{jm}]] \}. \quad \text{(A7)}$$

We dropped, as usual, the isospin indices except under the summation sign and in the amplitudes. We also introduced the following shorthand notations

$$x_\tau(\lambda_2 k\alpha_4 n; m\gamma_2; c_2) = W(\lambda_2 k\alpha_4 n; m\gamma_2)\overline{X}_\tau(kn; c_2\gamma_2),$$
$$y_\tau(lkij; \lambda_2\gamma_2; c_2) = W(lkij; \lambda_2\gamma_2)\overline{Y}_\tau(jk; c_2\gamma_2). \quad \text{(A8)}$$

Here $W(abcd;ef)$ denotes the Racah coefficient. In deriving Eq. (A7) we neglected the YY products, because one has $|Y/X| \leqslant 0.2$. Our calculations showed that the contribution of the last lines containing y terms in Eq. (A7) is small.

[1] D. J. Rowe, *Nuclear Collective Motion* (Methuen, London, 1970).
[2] P. Ring and P. Schuck, *The Nuclear Many-Body Problem* (Springer-Verlag, Berlin, 1980).
[3] R.F. Casten and N.V. Zamfir, Phys. Rep. **264**, 81 (1996).
[4] D.R. Bes and R.A. Broglia, Nucl. Phys. **80**, 289 (1966).
[5] R.A. Broglia, V. Paar, and D.R. Bes, Phys. Lett. **37B**, 159 (1971); **37B**, 257 (1971).
[6] D.R. Bes and G.G. Dussel, Nucl. Phys. **A135**, 1 (1969); **A135**, 25 (1969).
[7] R.A. Broglia and P.F. Bortignon, Phys. Lett. **65B**, 221 (1976).
[8] P. Ring and P. Schuck, Z. Phys. **269**, 323 (1974).
[9] P. Schuck, Z. Phys. A **279**, 31 (1976).
[10] R.J. Liotta and C. Pomar, Nucl. Phys. **A362**, 137 (1981); **A382**, 1 (1982).

[11] B. Silvester-Brac and R. Piepenbring, Phys. Rev. C **26**, 2640 (1982).
[12] K.V. Protasov, B. Silverster-Brac, R. Piepenbring, and M. Grinberg, Phys. Rev. C **53**, 1646 (1996).
[13] K.V. Protasov and R. Piepenbring, Nucl. Phys. **A632**, 39 (1998).
[14] A. Insolia, N. Sandulescu, J. Blomqvist, and R.J. Liotta, Nucl. Phys. **A550**, 34 (1992).
[15] N. Sandulescu, A. Insolia, B. Fant, J. Blomqvist, and R.J. Liotta, Phys. Lett. B **288**, 554 (1992).
[16] D.S. Delion and J. Suhonen, Phys. Rev. C **61**, 024304 (2000).
[17] V. G. Soloviev, *Theory of Atomic Nuclei: Quasiparticles and Phonons* (Institute of Physics, Bristol, 1992).
[18] V.G. Soloviev and N.Yu. Shirikova, Z. Phys. A **301**, 263 (1981).
[19] V.G. Soloviev, Ch. Stoianov, and A.I. Vdovin, Nucl. Phys. **A288**, 376 (1977).
[20] C.A. Bertulani and V.Yu. Ponomarev, Phys. Rep. **321**, 139 (1999).
[21] V.Yu. Ponomarev, P.F. Bortignon, R.A. Broglia, and V.V. Voronov, Phys. Rev. Lett. **85**, 1400 (2000).
[22] V.Yu. Ponomarev, P.F. Bortignon, R.A. Broglia, and V.V. Voronov, Nucl. Phys. **A678**, 170c (2001).
[23] V.G. Soloviev, A.V. Sushkov, N.Yu. Shirikova, and N. Lo Iudice, Nucl. Phys. **A600**, 155 (1996).
[24] F. Catara, Ph. Chomaz, and N. Van Giai, Phys. Lett. B **233**, 6 (1989).
[25] F. Catara, Ph. Chomaz, and N. Van Giai, Phys. Lett. B **277**, 1 (1992).
[26] E.G. Lanza, M.V. Andres, F. Catara, Ph. Chomaz, and C. Volpe, Nucl. Phys. **A636**, 452 (1998).
[27] M.V. Andres, F. Catara, E.G. Lanza, Ph. Chomaz, M. Fallot and J.A. Scarpaci, Phys. Rev. C **65**, 014608 (2001).
[28] I. Hamamoto, Phys. Rev. C **60**, 054320 (1999).
[29] G.F. Bertsch, P.F. Bortignon, and K. Hagino, Nucl. Phys. **A657**, 59 (1999).
[30] S. Drozdz, S. Nishizaki, J. Speth, and J. Wambach, Phys. Rep. **197**, 1 (1990).
[31] A. Klein and E.R. Marshalek, Rev. Mod. Phys. **63**, 375 (1991).
[32] D.S. Delion and J. Suhonen, Phys. Rev. C **64**, 064302 (2001).
[33] D. Bucurescu, G. Cata, D. Cutoiu, G. Constantinescu, M. Ivascu, and N.V. Zamfir, Z. Phys. A **324**, 387 (1986).
[34] L.E. Svensson *et al.*, Nucl. Phys. **A584**, 547 (1995).
[35] C. Fahlander *et al.*, Nucl. Phys. **A485**, 327 (1988).
[36] R.F. Casten *et al.*, Phys. Lett. B **297**, 19 (1992).
[37] H.H. Hsu, S.A. Williams, F.K. Wohn, and F.J. Margetan, Phys. Rev. C **16**, 1626 (1977).
[38] V.K. Datta, V.P. Varshney, K.K. Gupta, and S.P. Sud, J. Phys. Soc. Jpn. **54**, 901 (1985).
[39] K. Weeks and T. Tamura, Phys. Rev. C **22**, 888 (1980).
[40] P. van Isacker and G. Puddu, Nucl. Phys. **A384**, 125 (1980).
[41] J. Stachel, P. Van Isacker, and K. Heyde, Phys. Rev. C **25**, 650 (1982).
[42] J. Vervier and R.V.F. Janssens, Phys. Lett. **108B**, 1 (1982).
[43] R.F. Casten, Ch.-L. Wu, Da Hsuan Feng, J.N. Ginocchio, and X.-L. Han, Phys. Rev. Lett. **56**, 2578 (1986).
[44] J. Suhonen and O. Civitarese, Phys. Lett. B **497**, 221 (2001).
[45] A. Bohr and B. R. Mottelson, *Nuclear Structure* (Benjamin, New York, 1969), Vol. I.